

**BOLTED LAP JOINT MONITORING USING ULTRASONIC GUIDED WAVES
CONSIDERING TEMPERATURE VARIATIONS**

Xuezhi Peng

University of Michigan-Shanghai Jiao Tong
University Joint Institute, Shanghai Jiao Tong
University, Shanghai, China

Yanfeng Shen

University of Michigan-Shanghai Jiao Tong
University Joint Institute, Shanghai Jiao Tong
University, Shanghai, China;
Shanghai Key Laboratory for Digital
Maintenance of Buildings and Infrastructure,
Shanghai, China

ABSTRACT

This paper presents the numerical investigation of ultrasonic guided waves for bolted lap joint Structural Health Monitoring (SHM), considering temperature variations. It first systematically discusses the mechanisms behind the linear and nonlinear ultrasonic techniques for bolt loosening detection. Afterwards, a general Finite Element Model (FEM) of a bolted structure was established to observe and verify the influence of the change of bolt pre-tightening force on the linear and nonlinear characteristics of ultrasonic guided waves. In order to further study the effect of temperature variation on the sensing signals, the structure is subjected to various levels of thermal loads. This study examines the temperature influence on both linear and nonlinear signal features, such as the transmitted wave energy and the nonlinearity of waveforms. Simulation results show that an increment in temperature can cause partial detachment of the interface between two lap joint components in the structure, resulting in a decrease in both the linear energy and the degree of nonlinear higher-order harmonics. The paper finishes with concluding remarks and suggestions for future work.

Keywords: bolt loosening; temperature compensation, nonlinear ultrasonics; structural health monitoring; nondestructive evaluation; guided waves

1. INTRODUCTION

Due to the easy implementation and low cost, bolted joints, as the main type of detachable connection, have been widely used in a large family of industrial fields such as machinery, civil, and aerospace engineering. For safety reasons, bolted connections must meet strict durability, reliability and integrity

standards. Because of improper installation [1], dynamic load and corrosion [2], bolt loosening often occurs and seriously threatens the safety of engineering infrastructures. Therefore, continuous monitoring and accurate detection of bolt looseness is critical to ensure structural safety.

In the past, researchers have proposed various methods for monitoring and detecting bolt looseness. Structural Health Monitoring (SHM) technology based on ultrasonic guided waves has been applied in bolt loosening evaluation due to its wide detection range and high sensitivity [3,4]. Traditional ultrasonic nondestructive testing is based on linear dynamic theory [5,6]. The principle of this method is that the reduction of the pre-tightening force caused by the loosening of the bolt changes the properties of the contact surface, such as damping, stiffness, and actual contact area [7]. This results in changes in the parameters of the guided wave propagating through the interface, such as wave velocity, signal attenuation, transmission and reflection coefficients [8]. Therefore, the sensor can detect different responses after the wave passes through the contact surfaces. Jhang et al. used phase detection techniques to precisely measure the linear variation of the time-of-flight (TOF) of ultrasonic waves in the bolt under different preloads [9]. Yang and Chang proposed a method based on the energy decay to determine the location and degree of bolt loosening [10]. Parvasi et al. proposed a time-domain inversion technique based on the energy method to judge the bolt pre-tightening force by the peak value of the received signals [11].

Detection methods using linear signal features work well for severe bolt loosening, but these linear features may not be significant when the bolt is slightly loose [12]. To overcome this limitation of the linear methods, a nonlinear ultrasonic method

was proposed, and its effectiveness was proved by theoretical analysis and experimental verifications [13,14]. Nonlinear ultrasonic methods often rely on the interactions of excitation signal and the contact surfaces at the bolted joints. When a slight bolt loosening is present, these interactions can result in different frequencies of the sensing signal compared with the excitation signal [15]. Such a phenomenon is known as the Contact Acoustic Nonlinearity (CAN) [16]. The CAN theory is based on the fact that when a guided wave passes through a contact surface, the interface "breathing" motion pattern - manifested as the two contact surfaces closing during wave compression and opening during wave tension - lead to apparent stiffness variation during the cyclic loading. Thus, CAN introduces local nonlinearities into propagating waves guided by the medium [17]. Based on CAN theory, when the bolt is slightly loose, the received signal will show nonlinear characteristics in the spectrum, including high-order harmonics, subharmonics, and sidebands. Among the methods based on higher-order harmonics, the second-order and third-order harmonics have received extensive attention. Its occurrence and magnitude can be correlated with the presence and severity of CAN [17,18]. By observing the CAN of the connection, the bolt tightening condition can be evaluated qualitatively and quantitatively. Shen et al. used nonlinear ultrasonic spectroscopy simulations and experiments to prove that the CAN generated by the interaction between the guided waves and the contact surfaces can be used to assess bolt tightness [19]. Yan et al. utilized second-order harmonics to evaluate the tightness of bonded aluminum joints and minimized nonlinear effects unrelated to loosening [20]. Amerini and Meo used the second-order harmonic to evaluate the tightness of metal bolted structures and obtained remarkable results [21].

However, most of the bolt loosening detection techniques so far has been conducted at room temperature. Few studies devoted to the effect of ambient temperature variation on the bolt loosening diagnosis. Changes in temperature will impose different degrees of influences on various components of the bolted structure, resulting in changes in the characteristics of the sensing signals. Therefore, the influence of the ambient temperature cannot be ignored. This paper analyzes the mechanism behind the linear wave energy dispersion (WED) method and the nonlinear higher-order harmonic (HOH) method. The Finite Element Model (FEM) of the bolted structure is established to analyze the performance of the two methods under different bolt pre-tightening forces. The simulation adopts the pitch-catch method. Piezoelectric Wafer Active Sensors (PWASs) are used as the transmitter and receiver. Then, the thermal load is applied to the finite element model, and the influence of temperature change on the two methods is analyzed. This paper finishes with concluding remarks and future work.

2. THEORETICAL BACKGROUND AND PREVAILING METHODOLOGY

2.1 WED based linear theory for bolt loosening monitoring

From a microscopic point of view, the solid surface is rough and uneven, which leads to the fact that the actual contact area of two pieces of metal in contact with each other is smaller than their surface contact area. In a bolted construction, two connected parts are joint together, as shown in Figure 1a. If the bolt is tightened, the structure can be considered elastic. The relationship between the bolt pre-tightening force F and the torque T applied to the bolt can be estimated by [22]

$$F = \frac{T}{Kd} \quad (1)$$

where K is the friction coefficient between the bolt and nut and d represents the bolt diameter. The actual contact area between the two components in a bolted structure is determined by the torque applied to the bolt. The loosening of the bolt due to the reduced torque results in a reduction in the contact pressure at the contact surface and consequently a reduction in the contact area. The quantitative relationship between the torque of the bolt and the actual contact area can be derived by Hertzian contact theory [23].

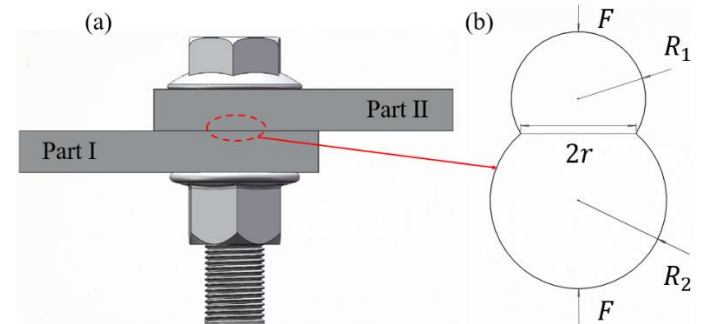


FIGURE 1: SCHEMATIC OF: (A) A BOLTED STRUCTURE; (B) HERTZIAN CONTACT MODEL.

In Hertzian contact theory, as shown in Figure 1b, two contact bodies with a small contact area are regarded as two elastic spheres with radii R_1 and R_2 , respectively. Under the bolt pre-tightening force F , the contact surface interpreted by two elastic spheres is squeezed together, and the radius r of their substantial contact area is given as

$$r = \left(\frac{R_1 R_2}{R_1 + R_2} \right)^{1/3} \left(\frac{3F(1 - \nu^2)}{4E} \right)^{1/3} \quad (2)$$

$$\frac{1 - \nu^2}{E} = \frac{1 - \nu_1^2}{E_1} + \frac{1 - \nu_2^2}{E_2} \quad (3)$$

where E is the Young's modulus and ν donates the Poisson's ratio, subscripts 1 and 2 for Part I and Part II. After that, the actual contact area S can be calculated by

$$S = \pi r^2 = \pi \left[\left(\frac{R_1 R_2}{R_1 + R_2} \right) \left(\frac{3(1 - \nu^2)}{4E} \right) \right]^{2/3} F^{2/3} \quad (4)$$

Then the elastic waves propagating in the bolted structure is analyzed. When the two bolted plates are thin, elastic waves propagate mainly in the form of Lamb waves. When propagating through the bolt, the incident Lamb wave in Part I will split into four parts [24]:

- (1) the evanescent wave that decays rapidly due to the friction of contact surfaces;
- (2) the reflected wave that propagates in the opposite direction to the incident wave in Part I;
- (3) the wave that continues to propagate in Part I along the direction of incidence; and
- (4) the wave that propagates through the bolt into Part II and continues to propagate.

The energy carried by the wave propagating into Part II can be represented by $W_{through}$, which is proportional to the substantial contact area S between the two planes, which yields

$$W_{through} \propto S \propto P^{2/3} \propto T^{2/3} \quad (5)$$

From Eq. 5, it can be concluded that, under the premise of constant incident energy, the amount that can transmit into Part II decreases as the bolt pre-tightening force drops. Therefore, the amount of energy received by the PWAS installed on the structural surface of Part II can be used as a criterion for judging bolt loosening.

2.2 HOH based nonlinear theory for bolt looseness monitoring

Unlike the energy transmission ability which mainly depends on the actual contact area between the structures, CAN and its induced HOH mainly depend on the contact stiffness nonlinearity of the interface [25]. When the contact surface is considered elastic, contact stiffness can be divided into linear stiffness K_1 and nonlinear stiffness K_2 . The value of the contact stiffness depends on the material properties and the amount of pressure exerted on the contact surface. When the structural material is kept constant, the contact stiffness can be viewed as a function of pressure. Through perturbation analysis, it can be expressed as [26]

$$K_1 = CF^m \propto F^m \propto T^m \quad (6)$$

$$K_2 = \frac{1}{2}mC^2F^{2m-1} \propto F^{2m-1} \propto T^{2m-1} \quad (7)$$

where C and m are two positive parameters depending on the contact properties of interfaces. In most materials and industrial applications, $m < 0.5$, which shows that K_1 increases with the increase of F , and at the same time K_2 decreases [26]. Therefore, the linear component of the ultrasonic wave propagating through the interface will increase with increasing pressure, while the nonlinear component will decrease.

Taking the second-order harmonic as an example, the degree of nonlinearity β can be expressed as the ratio of the maximum amplitude of the second-order harmonic to the maximum amplitude of the main frequency. Through perturbation analysis, β can be approximated as a function of stiffness K_1 and K_2 [26]:

$$\beta \propto \frac{K_2}{K_1^2} \propto F^{-1} \propto T^{-1} \quad (8)$$

From Eq. 8, it can be concluded that the sensing signal nonlinearity increases with a decreasing bolt pre-tightening force. Therefore, the nonlinearity of the received signal can be used as a criterion for judging bolt looseness.

3. FINITE ELEMENT MODEL OF A GENERAL BOLTED STRUCTURE FOR THE NUMERICAL INVESTIGATIONS

In this section, FEM simulations are performed to demonstrate the effect of different bolt pre-tightening force on the linear and nonlinear components of the signal.

3.1 Finite element model layout

As shown in the Figure 2, a general bolted structure model was constructed. The model consists of three parts, two aluminum perforated plates as the two parts being bolted and an steel block to simulate the bolt. The thin cylinder in the middle represents the threaded column and two thick cylinders represent the screw head and the nut. The meshes of the three parts were not merged together and were connected merely through the contact surface conditions and the applied external forces. The two aluminum plates possessed the same size (175-mm long, 50-mm wide, and 4-mm thick), the overlapping part formed a square with side length of 50 mm, the round hole located at the center of the square, and the diameter of the hole was 15 mm. The head and nut of the bolt were 4-mm thick and 25 mm in diameter. The distance between the inner surface of the screw head and the nut was 8mm, which was equal to the sum of the thickness of the two plates. The diameter of the threaded column was 9mm. A PWAS was connected to each of the two aluminum plates, which were used to transmit and receive ultrasonic wave signals, represented as T-PWAS and R-PWAS, respectively. The PWAS took a cylindrical shape with a diameter of 3.5 mm and a thickness of 0.2 mm.

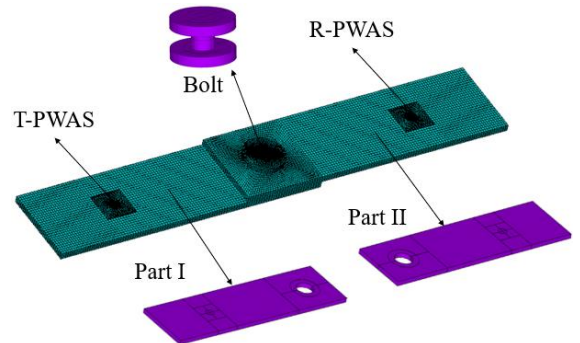


FIGURE 2: EXPLODED VIEW OF BOLT STRUCTURE MODEL.

Three contact pairs are introduced into the model, located between the screw head and the upper plate, between the two plates, and between the lower plate and the nut. As shown in Figure 3, the contact pair between the plate and the bolt formed a ring area covered by the washer. The contact pair between the two plates was a square area with a circular hole. In each contact

pair, the upper surface is selected as the contact surface, represented by CONTA174 elements, and the lower surface is selected as the target surface, represented by TARGE170 elements. Excessive contact stiffness will cause convergence difficulty, so the contact stiffness penalty factor value was chosen to be 0.001. To avoid causing ill-conditioning and non-convergence, the extended Lagrange algorithm was selected as the contact algorithm. The friction coefficient of the contact surface was set to infinity to simulate a rough contact without sliding.

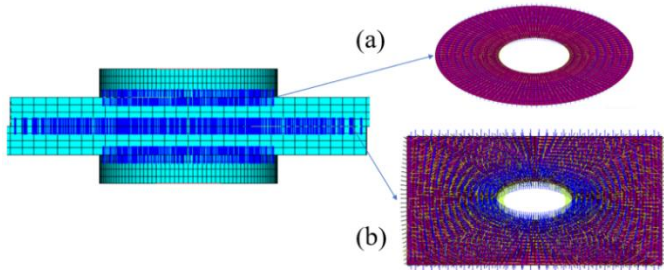


FIGURE 3: CONTACT PAIRS BETWEEN: (A) BOLT AND ALUMINUM PLATE; (B) TWO ALUMINUM PLATES.

After setting the contact pairs, an axial pressure load was applied to the area of the threaded column from the outer surface of the screw head and nut to represent the bolt tightening load, as showed in Figure 4. Since the entire bolt mesh was merged together, the pressure loaded on the threaded column was transferred to the head and nut and then to the aluminum plate through the contact surfaces. Through this process, the pressure loading of the entire structure was accomplished. The formula for calculating the pressure p was derived as follows,

$$p = \frac{F}{A} = \frac{4T}{\pi K d^3} \quad (9)$$

For steel bolts, the value of the friction coefficient K generally takes 0.2.

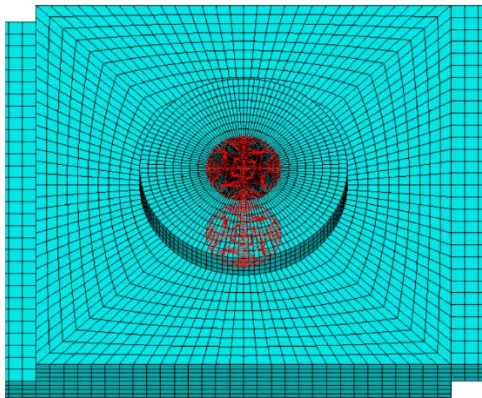


FIGURE 4: PRESSURE LOAD APPLIED TO THE THREADED COLUMN.

3.2 Simulation results showing the influence of bolt tightening force on the ultrasonic sensing signals

After establishing the FEM model, the coupled-field transient dynamic analysis was carried out. The T-PWAS was

excited by a 100 Vpp, 20-count tone burst, centered at 240 kHz. In order to ensure the temporal and spatial accuracy in depicting a sufficiently long signal, the time marching step size was set as 2×10^{-7} s, with a total number of 1000 steps. A total of five sets of case studies were carried out under different torque values, which are 0.05 Nm, 0.1 Nm, 0.3 Nm, 0.5 Nm and 1 Nm.

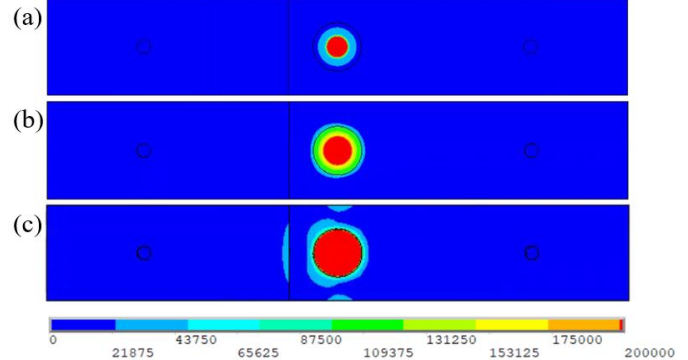


FIGURE 5: STATIC STRESS MAP OF THE STRUCTURE UNDER DIFFERENT BOLT PRE-TIGHTENING FORCES: (A) 0.1 Nm CASE; (B) 0.5 Nm CASE; (C) 1 Nm CASE.

Before the dynamic analysis, a step of static loading was performed first by turning off the time integration in the computation. The function of this step is to make the influence of pressure on the structure reach a steady state, so as to avoid the dynamic influence of pressure from propagating in the structure in the form of waves during the rest of the dynamic analysis. Thus, it was ensured that the signal received by the R-PWAS all come from the signal transmitted by the T-PWAS. The structure after static loading was shown in the Figure 5. The pressure range gradually expanded with the increase of the torque value.

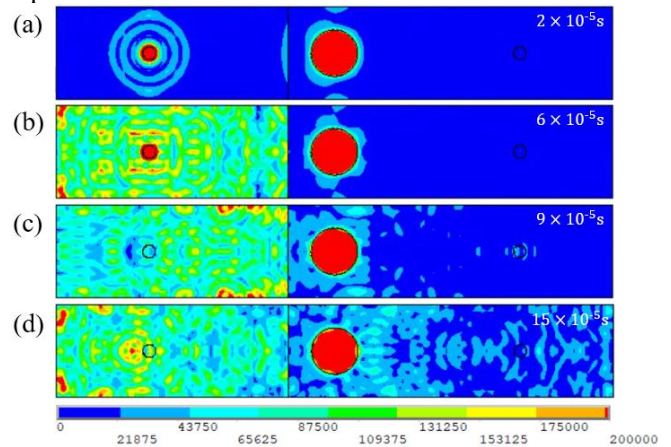


FIGURE 6: SNAPSHOTS OF WAVEFIELD IMAGES OF ULTRASONIC PROPAGATION IN THE BOLTED STRUCTURE.

Taking the case of 1 Nm torque load as an example, the four instances of ultrasonic propagation in the structure are shown in the Figure 6. First, the ultrasonic wave transmitted by T-PWAS started to diffuse in Part I. When the ultrasonic wave propagated to where the bolt was, it began to interact with the bolt. Then, the ultrasonic wave propagated through the contact surfaces into

Part II and reached the R-PWAS for the first time. Finally, after transmission and reflections, ultrasonic wave resided in Part II in complex forms.

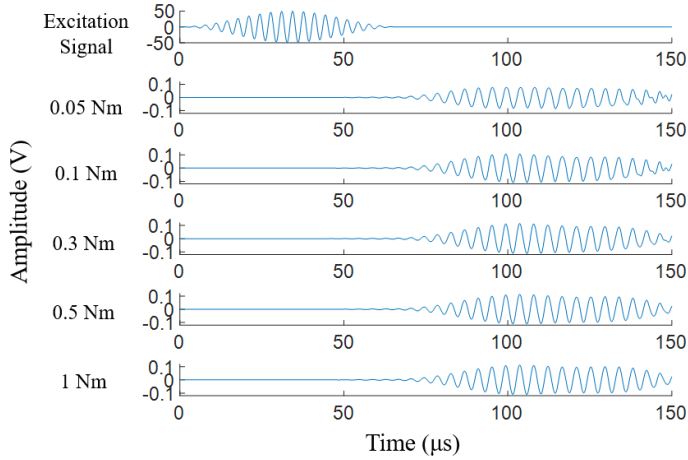


FIGURE 7: EXCITATION SIGNAL AND SENSING SIGNALS UNDER DIFFERENT BOLT PRE-TIGHTENING FORCES.

It can be noticed that transmission and multiple reflections were very obvious in the structure, so only the first wave packet arriving at the R-PWAS was selected to calculate the energy and nonlinearity of the sensing signals. The excitation signal and the originally received signals under different pre-tightening forces are presented in the Figure 7. After about 0.07 ms, the ultrasonic waves reached the R-PWAS. The received sensing waveforms resembled the excitation, and the overall amplitude increased slightly with the increment of the bolt tightness.

In order to extract the sensing signal features, the original signal needs to be post-processed. First, the signal was processed by a smoothing Hanning window to zero the beginning and end of the signal, so as to avoid DC noise interference caused by signal interception. The signal was then fast Fourier transformed (FFT) and high-pass filtered. The post-processed signal spectrum is shown in Figure 8.

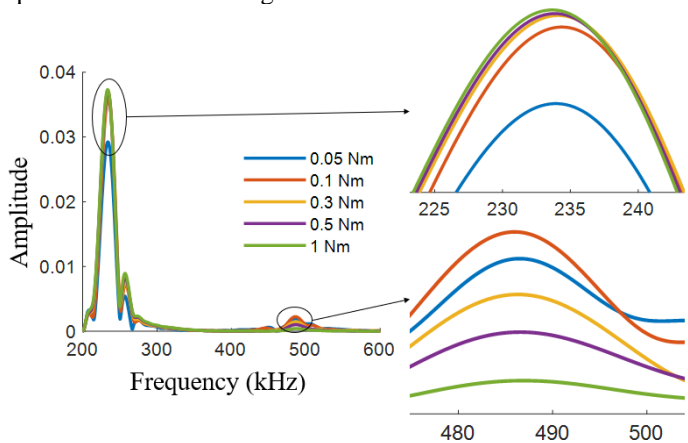


FIGURE 8: SIGNAL SPECTRUM UNDER DIFFERENT BOLT PRE-TIGHTENING FORCES.

It can be seen from the spectrum that the dominant frequency component of the signal increased as the bolt torque

grew, while the second-order harmonic decreased at the same time. The frequency domain area integration of the dominant frequency component was used to represent the wave energy. The ratio between the maximum amplitude of the second-order harmonic and the maximum amplitude of the dominant frequency served to evaluate the signal nonlinearity. The indexing trend is shown in Figure 9. It can be seen that the signal energy increased with the growth of the pre-tightening force value, while the signal nonlinearity dropped accordingly. The simulation results were in good agreement with the theoretical reasoning as presented in Section 2.

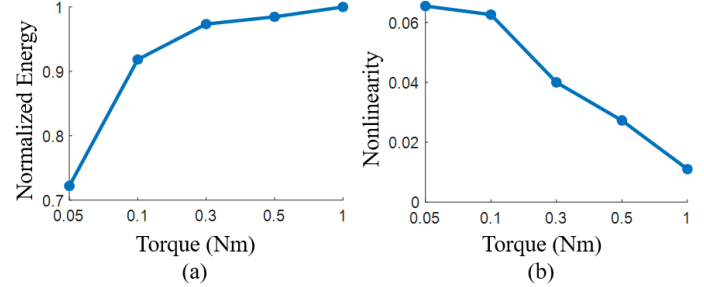


FIGURE 9: VARIATION TREND FOR (A) ENERGY AND (B) SECOND-ORDER HARMONIC NONLINEARITY WITH BOLT PRE-TIGHTENING FORCE.

4. TEMPERATURE VARIATION INFLUENCE ON THE SENSING SIGNAL FEATURES

In this section, FEM simulations are performed to investigate the effect of temperature variation on the bolt structure and ultrasonic wave propagation. On the basis of the above model, the thermal coefficients of various materials, such as the thermal expansion coefficient and the thermal conductivity, were introduced. At the same time, the same temperature load was applied to all nodes of the entire model to simulate the change of ambient temperature. In this simulation, a total of six comparative case studies of various temperature changes were carried out on the basis of 0.1 Nm bolt pre-tightening force: 0 °C (no temperature change), 0.5 °C, 1 °C, 2 °C, 5 °C and 10 °C.

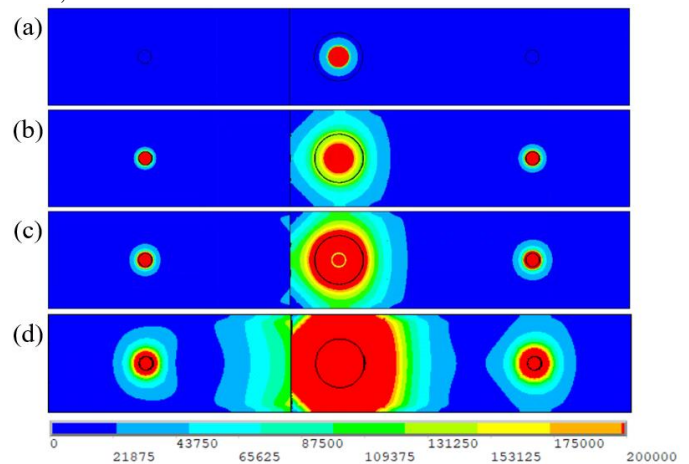


FIGURE 10: STRESS STATES DUE TO STATIC THERMAL LOADINGS WITH DIFFERENT TEMPERATURE VARIATIONS: (A) 0 °C CASE; (B) 0.5 °C CASE; (C) 2 °C CASE; (D) 5 °C CASE.

After the static loading was completed, it can be clearly seen from Figure 10 that the stress of the whole structure had changed dramatically due to the introduction of the thermal load. The stress at the contact part of the bolt was greatly enhanced, and the coverage also greatly increased. At the same time, stress also appeared in the contact area between the PWAS transducers and the aluminum plate, and it increased with the increment of the temperature variation. The reason for this phenomenon was that the entire structure was made of three different materials. The thermal expansion coefficient of aluminum is $2.4 \times 10^{-5} \text{ }^\circ\text{C}^{-1}$, the thermal expansion coefficient of steel is $1.2 \times 10^{-5} \text{ }^\circ\text{C}^{-1}$, and the thermal expansion coefficient of the piezoelectric ceramics is $0.9 \times 10^{-5} \text{ }^\circ\text{C}^{-1}$. The different values of thermal expansion coefficient lead to different deformation levels of each structural component under the same temperature change, which made the expansion of the aluminum plate larger than that of the steel bolt and the PWAS. Because the PWAS and the aluminum plate are merged together, the difference in the deformation was directly converted into the thermal stresses. Although the aluminum plate and the bolt were not merged together, due to the interactive contact constrains, the expansion would not have enough space and was also confined into thermal. The thermal stress showed a linear proportional behavior with respect to the amount of temperature change.

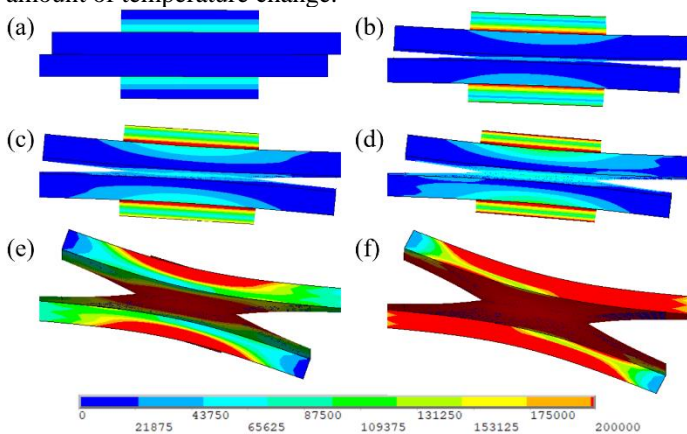


FIGURE 11: SCALED DEFORMATION OF THE BOLTED STRUCTURE AT DIFFERENT TEMPERATURE CHANGES: (A) 0 °C CASE; (B) 0.5 °C CASE; (C) 1 °C CASE; (D) 2 °C CASE; (E) 5 °C CASE; (F) 10 °C CASE.

After the deformation amount was scaled up by 10,000 times, the huge influence of temperature change on the contact surface of the bolt can be clearly seen from the side view of the structure. As shown in Figure 11, at the reference temperature, the contact surface of the upper and lower aluminum plates was completely fitted. After the thermal load was applied to the structure, the contact surface outside the bolt area became detached and warped around. With the increase of the thermal load, the area closely surrounding bolt also appeared to be detached to a certain extent, and the degree of warping also gradually increased.

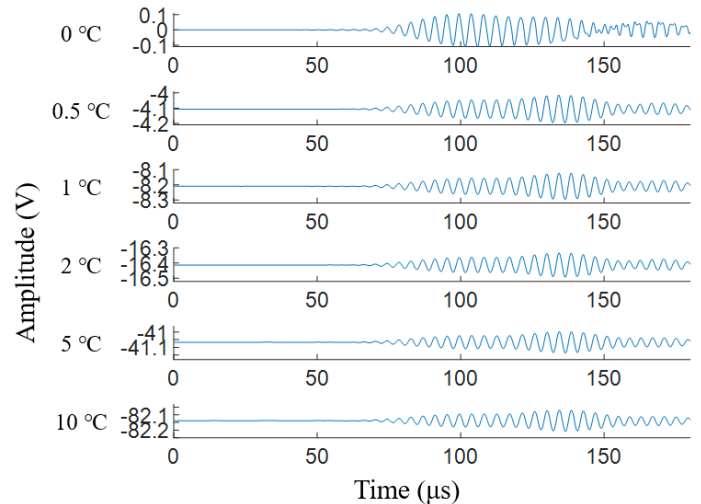


FIGURE 12: SENSING SIGNAL WAVEFORMS WITH DIFFERENT TEMPERATURE CHANGES.

This phenomenon was also reflected in ultrasonic wave propagation signals. The thermal stress between the PWAS and the aluminum plate lead to the accumulation of electrical charges on the surface of the PWAS, resulting in a DC component in the received signal, the magnitude of which was proportional to the thermal stress, as presented in Figure 12. In the practical applications, the accumulated charge would dissipate in the air, but in the ideal situation of the simulation, this part of the charge will always exist on the PWAS terminals. In order to eliminate the interference of the DC component, the signal was differentially processed. The frequency spectrum after the signal post-processing is shown in the Figure 13.

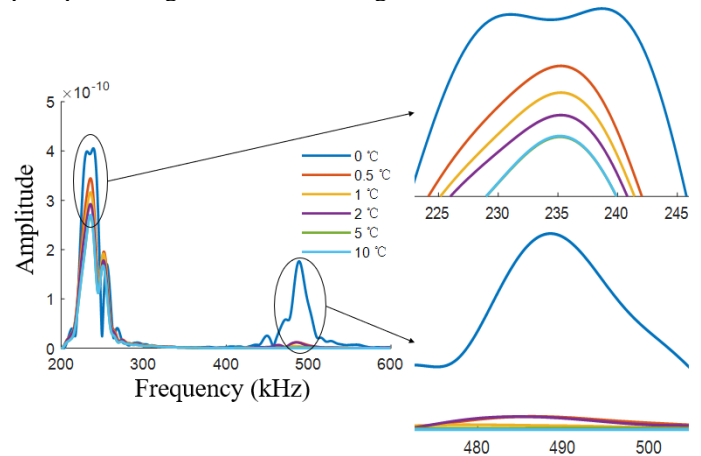


FIGURE 13: SIGNAL SPECTRA UNDER DIFFERENT TEMPERATURE CHANGES.

As can be seen from Figure 13, when the temperature increased, the amplitude of the main frequency component and its energy decreased, and the amplitude of second-order harmonic also decreased. Although the existence of thermal stress would lead to an increment in the degree of bolt tightening, this was inconsistent with the effect of increasing the torque. The reason for the decrease in the wave energy is that the contact

surfaces are disengaged due to thermal stress. Although the increase in bolt tightness will lead to an increment in the actual contact area of the two plates within the bolt action range, the detachment of the contact surface outside the bolt action range results in a substantial reduction in the actual contact area. The decrease was greater than the increase, resulting in the shrinking in the total contact area and a decrement in the total energy reaching the R-PWAS through the bolt. In terms of nonlinearity, although the strength of the second-order harmonic depends on the contact stiffness of the contact surface, the contact stiffness was also different due to the different pressures experienced by different regions in the entire contact surface. In the absence of the thermal load, the pressure and contact stiffness of the contact surface decreased gradually from the center of the bolt outward. The nonlinear component of the signal was mainly generated by the low contact stiffness part of the contact surface edge. After introducing the thermal load, the low contact stiffness part was completely detached, and the two plates were only connected by the part with high contact stiffness. Therefore, while the energy transfer was reduced, the nonlinearity of the ultrasonic wave was also substantially reduced.

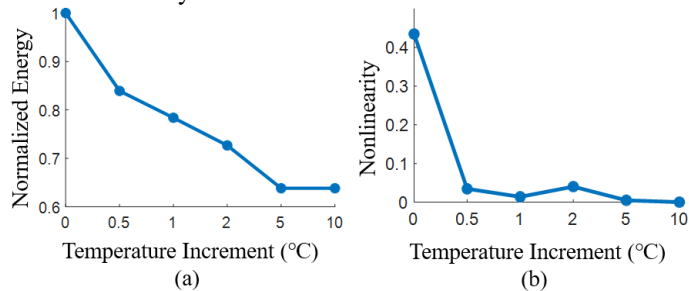


FIGURE 14: VARIATION TREND FOR (A) ENERGY AND (B) SECOND-ORDER HARMONIC NONLINEARITY WITH TEMPERATURE VARIATIONS.

It can be seen from the Figure 14 that when the temperature increment was small, the energy reduction of the signal formed an approximately first order polynomial relationship with the thermal load. When the temperature increment was greater than 5 °C, the received energy was almost unchanged, indicating that a steady state had been reached at this time: the part of the contact surface that can be disengaged had been completely detached, while the bolt and plate had been fully compressed. In terms of nonlinearity, the introduction of a small thermal load would lead to a large decrease in nonlinearity, which meant that the detachment of the contact surface edge would make it difficult for nonlinear components to appear. As the thermal load kept increasing, the nonlinearity also showed a slow decreasing trend. Eventually, the nonlinear component almost disappeared when the temperature increment reached 10 °C.

5. CONCLUDING REMARKS AND FUTURE WORK

This paper investigated the effect of temperature increment on the bolt structure and ultrasonic wave propagation in it. Firstly, by means of the linear WED method and the nonlinear HOH method of SHM, the influence of the change of bolt pre-tightening force on the ultrasonic wave propagation was clarified

through mechanism research and FEM analysis. Subsequently, linear and nonlinear aspects of the sensing signals were examined under various torque loads. It was found that the transmitted energy showed an increasing trend with a growing pre-tightening force value, while the signal nonlinearity demonstrated a decaying trend. The thermal effects were further investigated by applying the static thermal loads on the structure, simulating the ambient temperature changes. It was found that the temperature variations would introduce thermal stresses and deformations within the bolted lap joint structures. Such an effect would further influence the ultrasonic guided waves propagating through the bolt structure. Although temperature increment can improve bolt tightening level, it did not show the same effect as merely increasing pre-tightening force. It can be concluded that the temperature variation cannot be ignored in the SHM of bolt looseness and should be carefully handled.

Future work will be devoted to verifying the effect of temperature variation on the ultrasonic wave propagation in the bolted structure using experiments. Cases studies are also desired to investigate situations with various material combinations of different bolt structures.

ACKNOWLEDGEMENTS

The support from the National Natural Science Foundation of China (contract number 51975357 and 51605284) is thankfully acknowledged. This work was also sponsored by the Shanghai Rising-Star Program (contract number 21QA1405100).

REFERENCES

- [1] T. Wang, G. Song, S. Liu, Y. Li, H. Xiao, "Review of Bolted Connection Monitoring," *International Journal of Distributed Sensor Networks*, vol. 9, no. 12, 2013.
- [2] L. Huo, C. Li, T. Jiang, H. Li, "Feasibility Study of Steel Bar Corrosion Monitoring Using a Piezoceramic Transducer Enabled Time Reversal Method," *Applied Sciences*, vol. 8, no. 11, pp. 2304-2304, 2018.
- [3] G. Song, H. Gu, and H. Li, "Application of the Piezoelectric Materials for Health Monitoring in Civil Engineering: An Overview," in *Biennial Conference on Engineering*, pp. 680-687, 2004.
- [4] W. Bo, H. Linsheng, C. Dongdong, L. Weijie, and S. Gangbing, "Impedance-Based Pre-Stress Monitoring of Rock Bolts Using a Piezoceramic-Based Smart Washer—A Feasibility Study," *Sensors*, vol. 2017, no. 2, pp. 250-, 2017.
- [5] Rose and L. Joseph, "A Baseline and Vision of Ultrasonic Guided Wave Inspection Potential," *Journal of Pressure Vessel Technology*, vol. 124, no. 3, pp. 273-282, 2002.
- [6] L. Ye, Y. Lin, Z. Su, and C. Yang, "Quantitative assessment of through-thickness crack size based on Lamb wave scattering in aluminium plates," *Ndt & E International*, vol. 41, no. 1, pp. 59-68, 2008.
- [7] V. Giurgiutiu and A. N. Zagari, "Characterization of Piezoelectric Wafer Active Sensors," *Journal of Intelligent Material Systems and Structures*, vol. 11, no. 12, 2000.
- [8] X. Li, M. Luo, C. Hei, G. Song, "Quantitative evaluation of debond in concrete-filled steel tubular member (CFSTM)

using piezoceramic transducers and ultrasonic head wave amplitude," *Smart materials & structures*, vol. 28, no. 7, pp. 75033-75033, 2019.

[9] K. Y. Jhang, H. H. Quan, J. Ha, and N. Y. Kim, "Estimation of clamping force in high-tension bolts through ultrasonic velocity measurement," *Ultrasonics*, vol. 44 Suppl 1, no. 8, pp. e1339-42, 2006.

[10] J. Yang, and F.K. Chang, "Detection of bolt loosening in C—C composite thermal protection panels: II. Experimental verification," *Smart Materials and Structures*, vol. 15, no. 2, pp. 591–599, 2006.

[11] S. M. Parvasi, S. C. M. Ho, Q. Kong, R. Mousavi, and G. Song, "Real time bolt preload monitoring using piezoceramic transducers and time reversal technique—a numerical study with experimental verification," *Smart Materials and Structures*, vol. 25, no. 8, p. 085015, 2016.

[12] Z. Su, Z. Chao, H. Ming, C. Li, W. Qiang, and X. Qing, "Acousto-ultrasonics-based fatigue damage characterization: Linear versus nonlinear signal features," *Mechanical Systems & Signal Processing*, vol. 45, no. 1, pp. 225-239, 2014.

[13] Y. Shen and V. Giurgiutiu, "Predictive modeling of nonlinear wave propagation for structural health monitoring with piezoelectric wafer active sensors," *Journal of Intelligent Material Systems and Structures*, vol. 25, no. 4, pp. 506–520, 2014.

[14] K. Y. Jhang, "Nonlinear ultrasonic techniques for nondestructive assessment of micro damage in material: A review," *International Journal of Precision Engineering & Manufacturing*, vol. 10, no. 1, pp. 123-135, 2009.

[15] J. H. Parker, E. F. Kelly, and D. I. Bolef, "An Ultrasonic-Optical Determination of the Third Order Elastic Constant c_{111} for NaCl Single Crystals," *Applied Physics Letters*, vol. 5, no. 1, pp. 7-9, 1964.

[16] D. Donskoy, A. Sutin, and A. Ekimov, "Nonlinear acoustic interaction on contact interfaces and its use for nondestructive testing," *NDT & E International*, vol. 34, no. 4, pp. 231-238, 2001.

[17] M. H. A. B, Z. S. A. B, Q. W. C, L. C. A. B, and X. Q. D, "Modeling nonlinearities of ultrasonic waves for fatigue damage characterization: Theory, simulation, and experimental validation," *Ultrasonics*, vol. 54, no. 3, pp. 770-778, 2014.

[18] C. Zhou, Z. Su, L. Cheng, "Quantitative evaluation of orientation-specific damage using elastic waves and probability-based diagnostic imaging," *Mech. Syst. Signal Process*, pp. 2135–2156, 2011.

[19] Y. Shen, J. Bao, and V. Giurgiutiu, "Health Monitoring of Aerospace Bolted Lap Joints Using Nonlinear Ultrasonic Spectroscopy: Theory and Experiments," in *9th International Workshop on Structural Health Monitoring*, 2013.

[20] D. Yan, B. W. Drinkwater, and S. A. Neil D, "Measurement of the ultrasonic nonlinearity of kissing bonds in adhesive joints," *Ndt & E International*, vol. 42, no. 5, pp. 459-466, 2009.

[21] F. Amerini and M. Meo, "Structural health monitoring of bolted joints using linear and nonlinear acoustic/ultrasound

methods," *Structural Health Monitoring*, vol. 10, no. 6, pp. 659-672, 2010.

[22] J. Mínguez and J. Vogwell, "Effect of torque tightening on the fatigue strength of bolted joints," *Engineering Failure Analysis*, vol. 13, no. 8, pp. 1410-1421, 2006.

[23] B. Persson, "Contact mechanics for randomly rough surfaces," *Surface Science Reports*, vol. 61, no. 4, pp. 201-227, 2006.

[24] Zhang et al., "Quantitative evaluation of residual torque of a loose bolt based on wave energy dissipation and vibro-acoustic modulation: A comparative study," *Journal of Sound & Vibration*, 2016.

[25] I. Y. Solodov, "Ultrasonics of non-linear contacts: propagation, reflection and NDE-applications," *Ultrasonics*, vol. 36, no. 1-5, pp. 383-390, 1998.

[26] S. Biwa, S. Nakajima, and N. Ohno, "On the Acoustic Nonlinearity of Solid-Solid Contact with Pressure-Dependent Interface Stiffness," *Journal of Applied Mechanics*, vol. 71, no. 4, pp. 508-515, 2004.